Selected-ion flow tube studies of reactions of the radical cation $(HC_3N)^{+\bullet}$ in the interstellar chemical synthesis of cyanoacetylene

A. FOX, A. B. RAKSIT, S. DHEANDHANOO, AND D. K. BOHME[1]

Department of Chemistry and Centre for Research in Experimental Space Science, York University, Downsview, Ont. Canada M3J 1P3

Received August 15, 1985

A. FOX, A. B. RAKSIT, S. DHEANDHANOO, and D. K. BOHME. Can. J. Chem. **64**, 399 (1986).

The radical cation $(HC_3N)^{+\bullet}$ was produced in a Selected-Ion Flow Tube (SIFT) apparatus from cyanoacetylene by electron impact and reacted at room temperature in helium buffer gas with a selection of molecules including H_2, CO, HCN, CH_4, H_2O, O_2, HC_3N, C_2H_2, OCS, C_2H_4, and C_4H_2. The observed reactions exhibited a wide range of reactivity and a variety of pathways including charge transfer, hydrogen atom transfer, proton transfer, and association. Association reactions were observed with CO, O_2, HCN, and HC_3N. With the latter two molecules association was observed to proceed close to the collision limit, which is suggestive of covalent bond formation perhaps involving azine-like N—N bonds. For HC_3N an equally rapid association has been observed by Buckley *et al.* with ICR (Ion Cyclotron Resonance) measurements at low pressures and this is suggestive of radiative association. The hydrogen atom transfer reaction of ionized cyanoacetylene with H_2 is slow while similar reactions with CH_4 and H_2O are fast. The reaction with CO fails to transfer a proton. These results have implications for synthetic schemes for cyanoacetylene as proposed in recent models of the chemistry of interstellar gas clouds. Proton transfer was also observed to be curiously unfavourable with all other molecules having a proton affinity higher than $(C_3N)^{\bullet}$. Also, hydrogen-atom transfer was inefficient with the polar molecules HCN and HC_3N. These results suggest that interactions at close separations may lead to preferential alignment of the reacting ion and molecule which is not suited for proton transfer or hydrogen atom transfer.

A. FOX, A. B. RAKSIT, S. DHEANDHANOO, et D. K. BOHME. Can. J. Chem. **64**, 399 (1986).

La réaction d'impact électronique sur le cyanoacétylène a permis de générer le radical cation $(HC_3N)^{+\bullet}$ dans un tube à écoulement, à ion sélectif; on l'a fait réagir, à la température ambiante et dans de l'helium agissant comme gaz tampon, avec diverses molécules comme le H_2, le CO, le HCN, le CH_4, le H_2O, le O_2, le HC_3N, le C_2H_2, le OCS, le C_2H_4, et le C_4H_2. Les réactions observées représentent un large éventail de réactivités et une grande diversité de voies réactionnelles, y compris les transferts de charge, d'atomes d'hydrogène et de protons ainsi que les réactions d'association. On a observé des réactions d'association avec le CO, le O_2, le HCN et le HC_3N. Dans les cas de ces deux dernières molécules, on a observé que les réactions d'association se produisent jusqu'à la limite des collisions et ceci suggère qu'il y a formation de liaisons covalentes impliquant peut-être des liaisons N—N du type azine. Dans le cas du HC_3N, Buckley *et al.* ont aussi observé une réaction d'association à l'aide de mesures ICR alors qu'ils opéraient à basses pressions; ces résultats suggèrent une association radiative. La réaction de transfert d'atomes d'hydrogène du cyanoacétylène avec le H_2 est très lente alors que des réactions semblables avec le CH_4 et le H_2O sont rapides. La réaction avec le CO ne produit pas de réactions de transfert de proton. Ces résultats ont des implications pour les schémas de synthèse du cyanocétylène qui ont été proposés dans des modèles récents de la chimie des nuages gazeux interstellaires. On a aussi observé que la réaction de transfert de proton n'est curieusement pas favorable avec aucune des autres molécules possédant une affinité protonique plus élevée que celle du $(C_2N)^{\bullet}$. De plus, le transfert d'un atome d'hydrogène est inefficace avec les molécules polaires HCN et HC_3N. Ces résultats suggèrent que les interactions, lorsque les séparations sont faibles, peuvent conduire à un alignement préférentiel de l'ion qui réagit et de la molecule, qui n'est pas approprié pour un transfert de proton ou d'un atome d'hydrogène.

[Traduit par le journal]

Introduction

The radical cation $(HC_3N)^{+\bullet}$ has been implicated as an intermediate in the chemical synthesis of cyanoacetylene in dense interstellar gas clouds rich in molecular hydrogen (1–3). Available models of the chemistry proceeding in such clouds presume a rapid hydrogenation as indicated by reaction [1].

[1] $(HC_3N)^{+\bullet} + H_2 \rightarrow H_2C_3N^+ + H^{\bullet}$

Cyanoacetylene can be formed if the product ion of the hydrogenation reaction recombines with electrons as in reaction [2]

[2] $H_2C_3N^+ + e \rightarrow HC_3N + H^{\bullet}$

or transfers a proton to a molecule X as in reaction [3].

[3] $H_2C_3N^{+\bullet} + X \rightarrow XH^+ + HC_3N$

Sources of the radical cation $(HC_3N)^{+\bullet}$ which have been adopted in the various chemical models for interstellar gas clouds include the reaction of ${C_3H_2}^{+\bullet}$ with atomic nitrogen (1–3), the protonation of $(C_3N)^{\bullet}$ by ions such as ${H_3}^+$ and HCO^+ (3), and the reaction of ${C_2H_2}^{+\bullet}$ with the $(CN)^{\bullet}$ radical (1). Also, laboratory evidence is available for the formation of $(HC_3N)^{+\bullet}$ by the reactions of C_2H_2 with CN^+ (4) and $(HCN)^{+\bullet}$ (5). Another loss process for $(HC_3N)^{+\bullet}$ that may compete with reaction [1] in dense interstellar clouds is the reaction with CO, which is the most abundant molecule in these environments next to H_2. This reaction has been presumed in one available model (6) to occur rapidly by proton transfer as indicated in reaction [4].

[4] $(HC_3N)^{+\bullet} + CO \rightarrow HCO^+ + {}^{\bullet}C_3N$

There appears to be no previous systematic laboratory study of the reactions of $(HC_3N)^{+\bullet}$. The study reported here was directed specifically towards an experimental elucidation of the kinetics and product distributions of the reactions with H_2 and CO that are important in the interstellar chemistry. However, it was also extended towards a more general investigation of the hydrogenation of $(HC_3N)^{+\bullet}$ in reactions of type [5] with substrates

[5] $(HC_3N)^{+\bullet} + XH \rightarrow H_2C_3N^+ + X^{\bullet}$

strates XH = H_2O, HCN, CH_4, C_2H_2, C_2H_4, and HC_3N. Of

---

[1] Author to whom correspondence may be addressed.

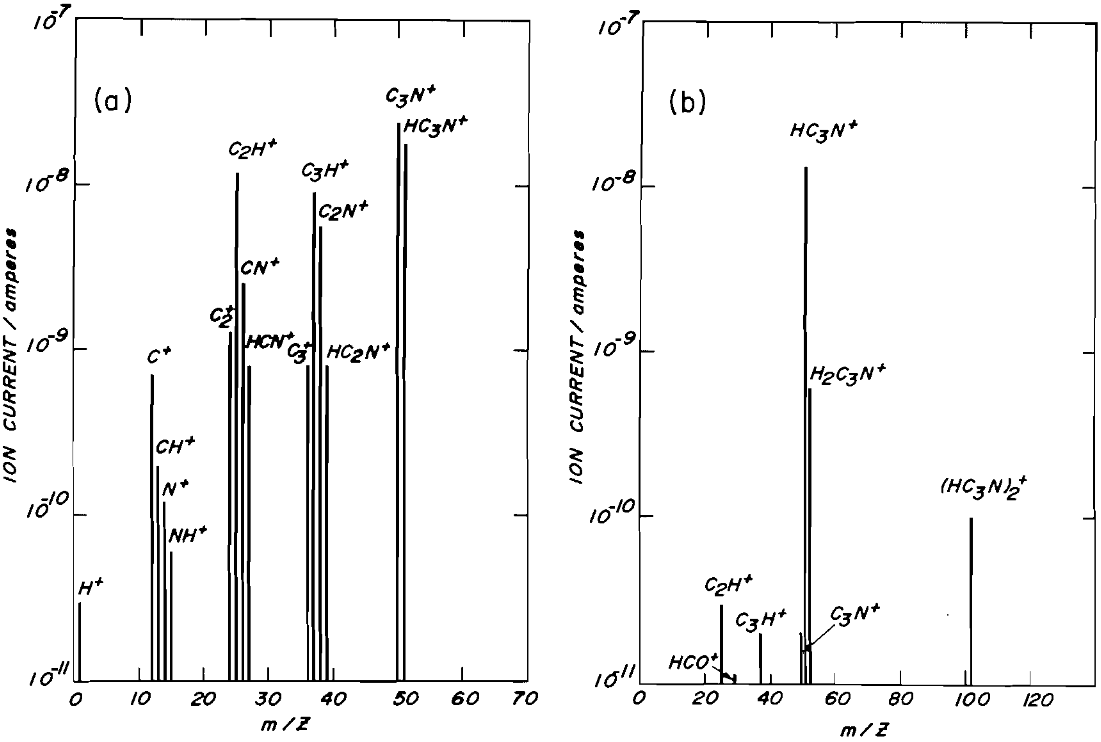

FIG 1. (a): SIFT spectrum for ions derived from cyanoacetylene (8% in helium) by electron impact at 28 eV. Ions are injected at 12 V; the buffer gas is helium at 0.315 Torr. (b): SIFT spectrum for HC_3N^+ derived from cyanoacetylene (10% in helium) by electron impact at 44.5 eV. The HC_3N^+ ions are injected at 12 V; the buffer gas is helium at 0.357 Torr. The background spectrum arises in part from ion–molecule reactions with water impurity and with cyanoacetylene leaking through the selection quadrupole.

additional interest was the competition of hydrogenation with charge transfer, which leads to the direct conversion of $(HC_3N)^{+\cdot}$ to cyanoacetylene as in reaction [6],

[6] $(HC_3N)^{+\cdot} + XH \rightarrow XH^{+\cdot} + HC_3N$

and the competition with proton transfer, as indicated by reaction [7],

[7] $(HC_3N)^{+\cdot} + XH \rightarrow XH_2^{+} + (C_3N)^{\cdot}$

which drives one of the proposed sources of $(HC_3N)^{+\cdot}$ in its opposite direction to regenerate the $(C_3N)^{\cdot}$ radical.

Experimental

The measurements were performed with the Selected-Ion Flow Tube (SIFT) apparatus in the Ion Chemistry Laboratory (7,8). The $(HC_3N)^{+\cdot}$ was generated in an axial electron impact ionizer (Extranuclear Model 0413) from cyanoacetylene diluted with helium at electron energies from 25 to 45 eV. The ions that may be derived from cyanoacetylene using this source are shown in Fig. 1, which also displays the spectrum downstream when $(HC_3N)^{+\cdot}$ is selected upstream. The major impurity ion is $H_2C_3N^+$, which is thought to arise primarily from the reaction of $(HC_3N)^{+\cdot}$ with H_2O impurity in the buffer gas, while the $(HC_3N)_2^{+\cdot}$ ion is presumed to arise from a rapid addition reaction with cycanoacetylene leaking from the source through the selection quadrupole. The ions were injected into helium buffer gas at ca. 12 V. The total pressure was in the range from 0.30 to 0.36 Torr (1 Torr = 133.3 Pa) and the ambient temperature was 296 ± 2 K. The reagent gases and vapours as well as the helium buffer gas were generally of high purity, with a minimum purity of 99.5 mol%. Hydrogen cyanide was prepared according to the procedure described by Glemser (9). The cyanoacetylene was prepared from methyl propriolate (Aldrich) (10). Chemical ionization of the hydrogen cyanide and cyanoacetylene using H_3^+ indicated a purity of greater than 99% for both of these reagents.

Results

Table 1 summarizes the rate constants and product distributions obtained in this study and includes values for the collision rate constant, k_c, for the reactions investigated (11). It includes all the primary product ions that were observed to contribute more than 5% to the total product spectrum. The reactions are listed in order of decreasing ionization energy of the neutral substrate. Rate constants were derived in the usual manner (7) and product distributions were determined using the method of Adams and Smith (12).

H_2

Hydrogen was observed to react with $(HC_3N)^{+\cdot}$ only slowly. Two primary products were observed, as is indicated in Fig. 2. The ion at $m/z = 26$ was assigned to be the acetylene cation $C_2H_2^{+\cdot}$ and not the vinylidene cation or CN^+. The formation of the latter is endothermic. Also, the $C_2H_2^{+\cdot}$ was observed to react further with H_2 to produce $C_2H_4^{+\cdot}$ and some $C_2H_3^+$ in the manner reported previously for the reaction of $C_2H_2^{+\cdot}$ derived by electron impact from acetylene (13). The data also provided an upper limit of 1×10^{-13} cm^3 $molecule^{-1}$ s^{-1} for the rate constants of the reactions of $C_2H_4^{+\cdot}$, $H_2C_3N^+$, and $(HC_3N)_2^{+\cdot}$ with H_2. The initial decay of the latter ion in Fig. 2 is due to the depletion of its source ion $(HC_3N)^{+\cdot}$.

CO

The measurement of the reaction of $(HC_3N)^{+\cdot}$ with CO was straightforward. The decay of $(HC_3N)^{+\cdot}$ provides an apparent second-order rate constant of 3.4×10^{-11} cm^3 $molecule^{-1}$ s^{-1} at a total pressure of 0.31 Torr. Only the adduct ion $(HC_3N)^{+\cdot}\cdot CO$ was observed to be present in the product ion spectrum. Proton transfer was not observed. The adduct ion and the impurity ions

TABLE 1. Summary of rate constants (in units of 10^{-9} cm^3 molecule^{-1} s^{-1}) and product distributions measured for reactions of $HC_3N^{+\bullet}$ with the SIFT technique at 296 ± 2 K

Neutral reactant	Products	Branching[a] ratio	k_{exp}[b]	k^c_c
H_2	$C_2H_2^{+\bullet} + HCN$	0.5	0.0019	1.5
	$H_2C_3N^+ + H^\bullet$	0.5		
CO	$(HC_3N)^{+\bullet}\cdot CO$	1.0	0.034[d]	0.80
HCN	$(HC_3N)^{+\bullet}\cdot HCN$	1.0	0.89[e]	3.3
CH_4	$C_2H_3N^{+\bullet} + C_2H_2$	0.5	0.59	1.1
	$C_3H_2N^+ + CH_3^\bullet$	0.3		
	$C_3H_4^{+\bullet} + HCN$	0.1		
H_2O	$H_2C_3N^+ + HO^\bullet$	1.0	0.67	2.4
O_2	$HCO^+ + (C_2NO)^\bullet$	0.4	0.0025[e]	0.67
HC_3N	$(HC_3N)^{+\bullet}\cdot HC_3N$	1.0	1.2[e]	3.4
C_2H_2	$C_4H_2^{+\bullet} + HCN$	0.8	0.64	1.0
	$C_2H_2^{+\bullet} + HC_3N$	0.2		
OCS	$(OCS)^{+\bullet} + HC_3N$	0.8	0.72	1.2
	$(HC_3NS)^{+\bullet} + CO$	0.2		
C_2H_4	$C_2H_4^{+\bullet} + HC_3N$	0.8	0.67	1.1
	$H_2C_3N^+ + C_2H_3^\bullet$	0.2		
C_4H_2	$C_4H_2^{+\bullet} + HC_3N$	1.0	0.89	1.1

[a] Primary product ions which contribute more than 5%. The branching ratio has been rounded off to the nearest 5% and is estimated to be accurate to ±30%.

[b] The accuracy of the rate constants is estimated to be better than ±30%.

[c] Collision rate constants derived from the combined variational transition state theory – classical trajectory study of Su and Chesnavich (11).

[d] In helium buffer gas at a total pressure of 0.31 Torr and concentration of 1.0×10^{16} atoms cm^{-3}.

[e] In helium buffer gas at a total pressure of 0.34 Torr and concentration of 1.1×10^{16} cm^{-3}.

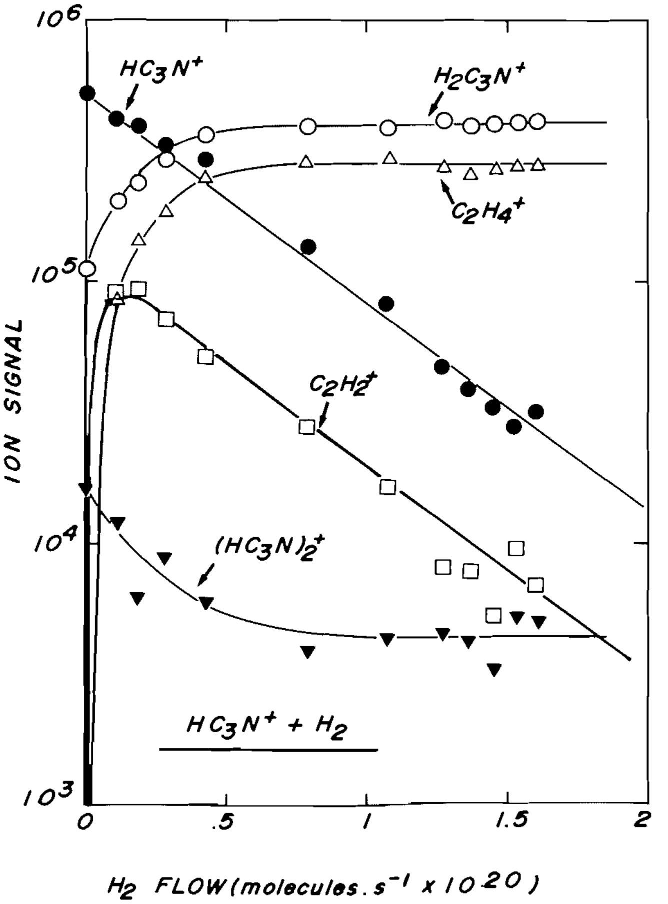

FIG. 2 The variations in ion signals recorded for the addition of hydrogen into the reaction region of the SIFT apparatus in which HC_3N^+ is initially established in helium buffer gas. $P = 0.341$ Torr, $\bar{v} = 7.0\times10^3$ cm s^{-1}, $L = 46$ cm, and $T = 297$ K. The HC_3N^+ is derived from cyanoacetylene at an electron energy of 44.5 eV and injected at 12 V.

$(HC_3N)_2^{+\bullet}$ and $H_2C_3N^+$ were all observed not to react with CO, $k \leq 1 \times 10^{-12}$ cm^3 molecule^{-1} s^{-1}.

HCN, HC_3N

Hydrogen cyanide and cyanoacetylene were observed to react with $(HC_3N)^{+\bullet}$ in a similar fashion. With both molecules adduct formation was predominant and rapid at the few tenths of a Torr of helium pressure employed in these measurements. Proton transfer was observed to be almost absent although the data analysis allowed for as much as about 5% of the reaction with HCN and about 1% of the reaction with HC_3N to proceed in this fashion. The product ion spectra provided evidence for the successive addition of up to three molecules of HCN and two molecules of HC_3N to $(HC_3N)^{+\bullet}$ but, interestingly, the addition of the first molecule was by far the most rapid in each case, by more than about an order of magnitude. Figure 3 displays data that illustrate this point for HC_3N.

CH_4

A variety of products was observed for the rapid reaction of ionized cyanoacetylene with methane. However, the stoichiometry is such that the product assignments were not straightforward. Product ions were observed at $m/z = 52$ ($H_2C_3N^+$ or $C_4H_4^+$), 41 ($H_3C_2N^+$ or $C_3H_5^+$), 40 ($H_2C_2N^+$ or $C_3H_4^+$), 28 (H_2CN^+ or $C_2H_4^+$), and 66 ($H_4C_4N^+$). Experiments with CD_4 allowed the exclusion of the following products: $C_4H_4^+$, $H_2C_2N^+$, and $C_2H_4^+$. Also an upper limit of 5% could be assigned to the formation of $C_3H_5^+$. Formation of $H_2C_3N^+$ can be ascribed to hydrogen atom transfer. The $H_4C_4N^+$ will arise from condensation with hydrogen atom elimination and may be protonated methylcyanoacetylene. The $C_3H_4^+$ will result from condensation followed by elimination of HCN and may also give rise to H_2CN^+ if proton transfer proceeds before the products separate. The nature of the $C_3H_4^+$ ion is uncertain. Available heats of formation suggest that ionized allene, methylacetylene, and *cis*-cyclopropane are some of the possibilities. The nature of the major product ion $H_3C_2N^+$ that may be formed by condensation with elimination of acetylene is also uncertain. A number of isomers can be thought to be formed. The heat of formation of ionized methyl cyanide is too high. Formation of ionized methyl isocyanide is less endothermic but still energetically unfavourable by 10 kcal mol^{-1}. Other isomers are possible, e.g. ionized ethynylimidogen, but their heats of formation are not known.

H_2O

The predominant channel observed for the reaction with H_2O was hydrogen atom transfer. Formation of C_3O^+, which cannot be distinguished from $H_2C_3N^+$ with our mass spectrometer, was excluded on the basis of experiments with D_2O. Less than 5% of the reaction proceeded by proton transfer and there was no evidence for charge transfer, which is endothermic in any case. The impurity dimer ion $(HC_3N)_2^{+\bullet}$ did not react with H_2O. A secondary reaction was observed between the $H_2C_3N^+$ and H_2O to form the adduct.

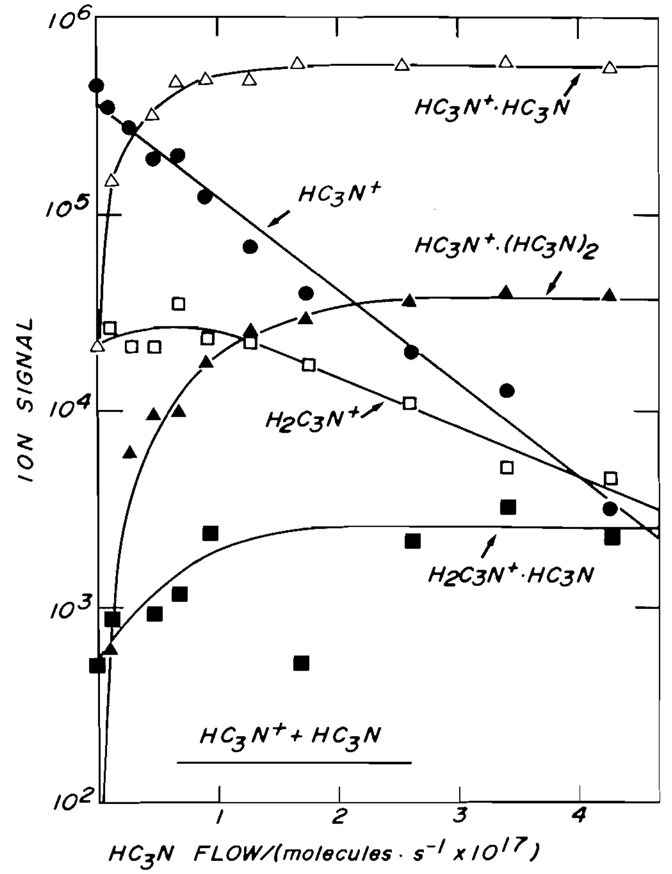

FIG. 3. The variations in ion signals recorded for the addition of cyanoacetylene into the reaction region of the SIFT apparatus in which HC_3N^+ is initially established in helium buffer gas. $P = 0.319$ Torr, $\bar{v} = 6.8 \times 10^3$ cm s^{-1}, $L = 46$ cm, and $T = 298$ K.

O_2

The reaction of $(HC_3N)^{+\cdot}$ with O_2 was the slowest reaction observed in this study with a measurable rate constant. HCO^+ and the adduct $(HC_3N)^{+\cdot}\cdot O_2$ were the only products observed and these were formed in approximately equal amounts.

C_2H_2

$C_2H_2^{+\cdot}$ and $C_4H_2^{+\cdot}$ appeared as the major product ions in this reaction. Formation of CN^+ and C_3N^+ is endothermic in this case. An abundance of secondary ion chemistry was observed since both of the primary product ions are reactive towards acetylene. We have established in separate experiments that $C_2H_2^{+\cdot}$ gives rise to $C_4H_2^{+\cdot}$, $C_4H_3^+$, and $C_4H_4^{+\cdot}$, which in turn add acetylene to give rise to the corresponding adduct ions. All of these conversions were observed to be initiated by the reaction of $(HC_3N)^{+\cdot}$ with acetylene. The $C_4H_3^+$ ion generated from $C_2H_2^{+\cdot}$, which also reacts further with acetylene, could not be distinguished with our mass spectrometer from $(HC_3N)^{+\cdot}$. Therefore it is conceivable that the decay of the ion at $m/z = 51$ provides only a lower limit to the rate constant of the primary reaction.

OCS

The predominant reaction observed with carbonyl sulphide was charge transfer, and the $(OCS)^{+\cdot}$ product ion reacted further to add one molecule of carbonyl sulphide. A minor channel was observed that corresponds to sulphur atom abstraction and so leads to the incorporation of sulphur into the cyanoacetylene ion. No reaction was observed with the $H_2C_3N^+$ ion that was also present initially. This is not surprising since proton transfer is endothermic in this case.

C_2H_4

$C_2H_4^{+\cdot}$ was the predominant product with ethylene and it rapidly reacted further to establish $C_3H_5^+$ and the adduct $(C_2H_4)_2^{+\cdot}$. The minor channel leading to the formation of $H_2C_3N^+$ corresponds to the transfer of a hydrogen atom.

C_4H_2

Charge transfer was the predominant reaction observed with diacetylene. The production of C_3N^+, which could not be distinguished with our mass spectrometer from $C_4H_2^{+\cdot}$, is endothermic. The $C_4H_2^{+\cdot}$ reacted further to form the adduct $C_4H_2^{+\cdot}\cdot C_4H_2$ as well as some $C_6H_2^{+\cdot}$. This latter reaction has been studied in separate experiments in more detail and will be reported elsewhere. It was also interesting to note that the $H_2C_3N^+$ reacted quite rapidly with diacetylene to add one molecule, while the addition of a second molecule was noted to be at least ten times slower. At 0.33 Torr of helium and a concentration of 1.1×10^{16} helium atoms cm^{-3} the apparent bimolecular rate constant for addition of the first molecule of diacetylene was $(8.7 \pm 2.6) \times 10^{-10}$ cm^3 $molecule^{-1}$ s^{-1}. This is close to the collision limit and probably reflects the formation of a strong hydrogen bond in the adduct. Bonding of the second diacetylene molecule would then be much less favourable and lead to a much lower rate of adduct formation.

Discussion and conclusions

The efficiency of the hydrogenation of ionized cyanoacetylene by H atom transfer from H_2 according to reaction [1] has been established in the experiments reported here to be less than 0.05% at 296 K. The hydrogen atom transfer is more than 30 kcal mol^{-1} exothermic but its low efficiency suggests that it has a positive activation energy. Consequently it may not contribute significantly to the formation of $H_2C_3N^+$ at the much lower temperatures found in interstellar gas clouds. The reactions with CH_4 and H_2O provide more efficient routes for the hydrogenation of ionized cyanoacetylene and so may be more suited to the eventual synthesis of cyanoacetylene by reactions [2] and [3]. Of course other reactions operate in interstellar gas clouds to establish $H_2C_3N^+$ without $HC_3N^{+\cdot}$ as a precursor, such as, for example, the reaction of $C_3H_3^+$ with N atoms (2, 3) and the reaction of $C_2H_2^{+\cdot}$ with HCN (5).

Also, we have shown that proton transfer from ionized cyanoacetylene to carbon monoxide does not occur at room temperature and so is not a viable reaction in models of the chemistry of interstellar clouds. We have observed a slow addition reaction in a few tenths of a Torr of helium to form what may be the isocyanate ion, $H{-}C{\equiv}C{-}C^{\cdot}{=}N^+{=}C{=}O$, but it is uncertain to what degree this happens in interstellar clouds in which radiative association would be the only means of stabilizing the adduct ion.

The reaction of ionized cyanoacetylene with carbonyl sulphide also has interesting implications for interstellar chemistry. The $(HC_3NS)^{+\cdot}$ ion formed in 20% of the reaction at room temperature is a potential source of $^{\cdot}S{-}C{\equiv}C{-}C{\equiv}N$ or $:C{=}C{=}C{=}N{-}S^{\cdot}$, which may be formed by the recombination of $(HC_3NS)^{+\cdot}$ with electrons.

The failure to observe significant amounts of proton transfer with any of the neutral reagents is curious. The proton affinities of the neutral molecules chosen as reagents span a range from 101 for H_2 to 184 kcal mol^{-1} for cyanoacetylene (14,15). The proton affinity of $(C_3N)^{\bullet}$ can be calculated to be 140 kcal mol^{-1} from the known heats of formation of ionized cyanoacetylene, the proton, and the $(C_3N)^{\bullet}$ radical. The latter is based on the appearance potential of CN^- from dicyanoacetylene (16) and appears to be reliable. The proton affiinity of $(C_3N)^{\bullet}$ is therefore less than that for CO (142), OCS (151), C_2H_2 (153), C_2H_4 (163), H_2O (166), HCN (171), C_4H_2 (180), and HC_3N (184), where the proton affinity is given in parentheses in kcal mol^{-1}. Yet the proton transfer observed with any of these molecules was at most 5% of the total reaction pathway.

Charge transfer, H atom transfer, and adduct formation were the alternate channels that appeared to compete successfully with proton transfer. The recombination energy of $(HC_3N)^{+\bullet}$ is 11.60 eV, which exceeds the ionization energy of the molecules C_4H_2 (10.17), C_2H_4 (10.5), OCS (11.18), and C_2H_2 (11.41). Charge transfer is therefore exothermic and indeed was observed to be a predominant reaction channel for each of these four molecules. For the reaction with C_2H_2 the ultimate formation of the charge transfer product is minor but we speculate that $C_2H_2^{+\bullet}$ in part also reacts with HC_3N before the products separate to produce $C_4H_2^{+\bullet}$. We have shown in a separate study that this latter reaction proceeds readily when $C_2H_2^{+\bullet}$ is produced by electron impact from acetylene (17).

The hydrogen atom affinity of ionized cyanoacetylene is at least 10 kcal mol^{-1} higher than the homolytic X—H bond energy of any of the molecules of type XH chosen as reagents in this study. Yet hydrogen atom transfer was observed not to compete effectively with charge transfer when the latter was also exothermic, as for the reactions with ethylene, acetylene, and diacetylene. Also it did not compete significantly with adduct formation for the reactions with HCN and HC_3N. In fact, only for the reactions with H_2, CH_4, and H_2O was hydrogen atom transfer observed to compete effectively with other reaction channels.

We suggest that both the curious failure of proton transfer and the discriminating behaviour of hydrogen atom transfer may be accounted for by steric constraints that could operate at close separations because of the electrostatic interaction between the cyanoacetylene ion and the reacting molecule. Preferential attack at the nitrogen end of the lengthy $(H{-}C{\equiv}C{-}C{\equiv}N)^{+\bullet}$ ion would put the proton "out of reach" of the reacting molecule and so prevent proton transfer. Also, for hydrogen atom transfer, the hydrogen atom in the reacting molecule may become "out of reach" of the ion, depending on the length and preferred alignment of the reacting molecule. This is likely to be the case with HCN and HC_3N, for example. These strong dipoles are likely to approach the positive ion preferentially with their negative nitrogen end. Azine type N—N bonding would then be possible if the nitrogen end of the ion is the site of attack. The high rates of association observed for the reactions with HCN and HC_3N are consistent with this kind of chemical bond formation. The linkages may be the type shown in [8] and [9].

[8] $H{-}C{\equiv}C{-}C^{\bullet}{=}N{-}N{=}C^{+}{-}H$

[9] $H{-}C{\equiv}C{-}C^{\bullet}{=}N{-}N{=}C^{+}{-}C{\equiv}C{-}H$

Adduct formation was not observed with H_2, H_2O, and CH_4 because the hydrogen atom in these molecules is easily "within reach." Adduct formation was also not observed with C_2H_2, C_2H_4, and C_4H_2. In these cases charge transfer is preferred because of the relatively low ionization potentials of these molecules.

The association of cyanoacetylene molecules with ionized cyanoacetylene has also just recently been observed by Buckley *et al.* in an ICR (Ion Cyclotron Resonance) and a high pressure photoionization mass spectrometer (18). The apparent bimolecular rate constant that was reported for the addition of the first molecule in the ICR at a total pressure of 10^{-6} Torr is surprisingly large, $k = 7.4 \times 10^{-10}$ cm^3 $molecule^{-1}$ s^{-1}, and close to the value obtained at the much higher pressures of the SIFT experiments reported here. High rates of association under SIFT conditions are normally attributable to the formation of strongly bound adducts stabilized by collision with the buffer gas atoms. In this case, however, the almost equally high specific rate observed at the much lower pressures of the ICR suggests that this stabilization may proceed by the emission of a photon and so implies a truly bimolecular radiative association reaction. Buckley *et al.* (18) have also proposed several bonding possibilities for the association reaction other than the azine-like linkage discussed earlier. They have pointed out that C—C bonding could lead to an ion of type [10] while C—N bonding may result in an ion of type [11]. These alternatives are attractive in that addition of a second molecule of cyanoacetylene to these dimer ions can lead to some interesting cyclic structures (18).

[10] $^{+}CH{=}C(CN){-}CH{=}C^{\bullet}{-}CN$

[11] $HC_2{-}C({=}N)^{\bullet}{-}N{=}C^{+}{-}C_2H$

Acknowledgment

We thank the Natural Sciences and Engineering Research Council of Canada for financial support.

1. S. S. Prasad and W. T. Huntress. Astrophys. J. **239**, 151 (1980).
2. T. J. Millar and A. Freeman. Mon. Not. R. Astron. Soc. **207**, 425 (1984).
3. C. M. Leung, E. Herbst, and W. F. Huebner. Astrophys. J. Suppl. **56**, 231 (1984).
4. A. B. Raksit, H. I. Schiff, and D. K. Bohme. Int. J. Mass Spectrom. Ion Processes, **56**, 321 (1984).
5. H. I. Schiff, G. I. MacKay, G. D. Vlachos, and D. K. Bohme. *In* The Proceedings of the I.A.U. Symposium on Interstellar Molecules. *Edited by* B. H. Andrews. D. Reidel Publ. Co., Dordrecht. 1981. pp. 307–310.
6. E. Herbst. Astrophys. J. Suppl. **53**, 41 (1983).
7. G. I. MacKay, G. D. Vlachos, D. K. Bohme, and H. I. Schiff. Int. J. Mass Spectrom. Ion Phys. **36**, 259 (1980).
8. A. B. Raksit and D. K. Bohme. Int. J. Mass Spectrom. Ion Phys. **55**, 69 (1983).
9. O. Glemser. *In* The handbook of preparative inorganic chemistry. *Edited by* G. Brauer. Academic Press, New York. 1963. p. 658.
10. C. Moureu and J. C. Bongrand. Ann. Chim. (Rome), **14**, 47 (1920).
11. T. Su and W. J. Chesnavich. J. Chem.Phys. **76**, 5183 (1982).
12. N. G. Adams and D. Smith. J. Phys. B, **9**, 1439 (1976).
13. D. Smith and N. G. Adams. Chem. Phys. Lett. **47**, 383 (1977).
14. S. G. Lias, J. F. Liebman, and R. D. Levin. J. Phys. Chem. Ref. Data, **13**, 695 (1984).
15. A. B. Raksit and D. K. Bohme. Int. J. Mass Spectrom. Ion Processes, **57**, 211 (1984).
16. V. H. Dibeler, R. M. Reese, and J. L. Franklin. J. Am. Chem. Soc. **83**, 1813 (1961).
17. A. B. Raksit and D. K. Bohme. Can. J. Chem. **63**, 854 (1985).
18. T. J. Buckley, L. W. Sieck, R. Metz, and S. G. Lias. Int. J. Mass Spectrom. Ion Processes, **65**, 181 (1985).

Charge distributions and chemical effects. XL. Chemical bonds in benzenoid hydrocarbons

S. Fliszár, G. Cardinal, and N. A. Baykara
Département de Chimie, Université de Montréal, C.P. 6210, Succ. A, Montréal (Qué.), Canada H3C 3V1

Received June 26, 1985

S. Fliszár, G. Cardinal, and N. A. Baykara. Charge distributions and chemical effects. XL. Chemical bonds in benzenoid hydrocarbons. Can. J. Chem. **64**, 404 (1986).

Benzenoid hydrocarbons were examined using a bond energy scheme featuring the role of atomic charges. The latter were conveniently deduced from appropriate correlations between theoretical results and ^{13}C nuclear magnetic resonance shifts. Atomization energies calculated in this manner agree with their experimental counterparts to within 0.36 kcal mol^{-1} (average deviation). It appears that benzenoid hydrocarbons can be efficiently described in terms of *local* charge density properties. In the absence of any distinctive specific feature characterizing benzenoids, this particular description of chemical bonds ultimately results in a unifying genealogy smoothly relating to one another the various possible types of CC and CH bonds which are formed by sp^2 and sp^3 carbons.

S. Fliszár, G. Cardinal et N. A. Baykara. Charge distributions and chemical effects. XL. Chemical bonds in benzenoid hydrocarbons. Can. J. Chem. **64**, 404 (1986).

Utilisant un schéma d'énergie de liaison comportant le rôle des charges atomiques, on a étudié des hycrocarbures benzènoïdes. On peut facilement déduire les charges atomiques des corrélations appropriées entre les résultats théoriques et les déplacements chimiques du ^{13}C en rmn. Les énergies d'atomisation calculées de cette manière sont en accord, dans des limites de 0,36 kcal mol^{-1} (déviation moyenne). Il semble que les hydrocarbures benzènoïdes peuvent être décrits d'une manière efficace en fonction des propriétés de densité de charge *locale*. En l'absence de caractéristiques spécifiques distinctives des benzènoïdes, cette description particulière des liaisons chimiques resulte finalement en un généalogie reliant l'un à l'autre les divers types possibles de liaisons CC et CH formées par les carbones sp^2 et sp^3.

[Traduit par le journal]

Introduction

This study describes benzenoid hydrocarbons. It considers the role of electronic charges in chemical bonding and leads to reasonably accurate energy calculations using atomic charges deduced from ^{13}C nmr shifts. Moreover, it offers a vivid insight into the nature of chemical bonds.

The expression

$$[1] \qquad \epsilon_{ij} = \epsilon^0_{ij} + a_{ij}\Delta q_i + a_{jk}\Delta q_j$$

indicates how their energies depend on the charges of the bond-forming atoms (1–3): ϵ^0_{ij} is for a reference bond with net charges q^0_i and q^0_j at atoms i and j, respectively, whereas ϵ_{ij} corresponds to modified charges, $q_i = q^0_i + \Delta q_i$ and $q_j = q^0_j + \Delta q_j$. The a_{ij} and a_{ji} parameters, "measuring" the changes in bond energy accompanying unit charge variations at atoms i and j, respectively, are discussed further below, as well as the ϵ^0_{ij}'s. Finally, the sum[1]

$$[2] \qquad \Delta E^*_a \simeq \sum_{i<j} \epsilon_{ij}$$

is a valid approximation for the atomization energy of a molecule at its potential minimum. Indeed, the formula

$$[3] \qquad \Delta E^*_a \simeq \Sigma\epsilon^0_{ij} + \Sigma_i\Sigma_j a_{ij}\Delta q_i$$

has proven accurate in over 130 comparisons between calculated and experimental energies (Fig. 1).

Equation [3] indicates the steps involved in these energy calculations. We begin with a description of the appropriate a_{ij} and ϵ^0_{ij} parameters, which will be conveniently tabulated. Next, we discuss the derivation of the required Δq_i charges, with the help of ^{13}C nmr shifts. Then it becomes a simple matter of assembling the pieces in order to deduce ΔE^*_a and,

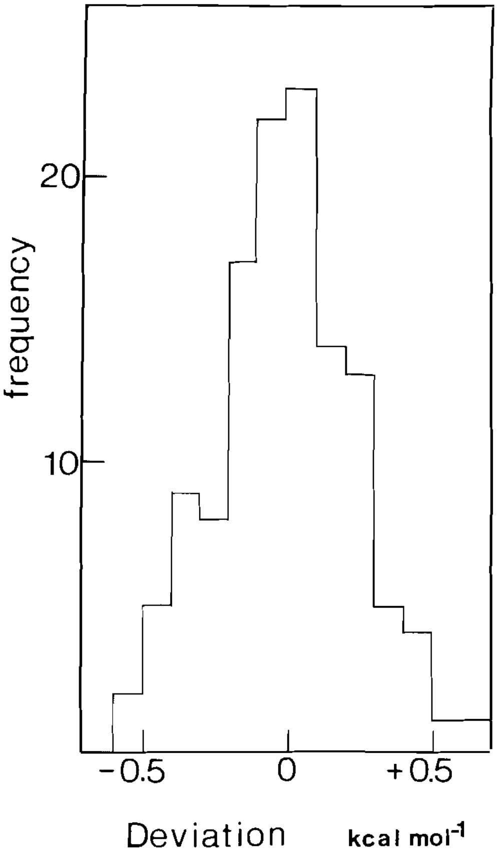

FIG. 1. Frequency of deviations between calculated and experimental atomization energies. This error distribution survey covers alkanes (1, 2) (including cycloalkanes constructed from chair and (or) boat cyclohexane rings), simple ethylenic (4) and polyunsaturated hydrocarbons (5), both conjugated and nonconjugated, as well as ethers, aldehydes, and ketones (6). The average deviation is ~0.23 kcal mol^{-1}.

---

[1] The omitted nonbonded contributions can safely be neglected in a first approximation (1–3).

TABLE 1. Most frequently used a_{ij} values[a], from eq. [4]

Bond	i—j	R_{ij} (Å)	a_{ij} (kcal mol^{-1} me^{-1})
1	C(Ar)—C(Ar)	1.40	$a_{CC}^{\sigma\cdot\pi} = -0.358$
2	C(sp^3)—C(sp^3)	1.53	$a_{CC} = -0.488$
3	C(Ar)—H	1.08	$a_{CH}^{\sigma\cdot\pi} = -0.083$
4	C(sp^3)—H	1.08	$a_{CH} = -0.247$
5	H—C	1.08	$a_{HC} = -0.632$
6	C(Ar)—C(sp^3)	1.53	$a_{CC}^{\sigma} = -0.450$
7	C(Ar)—H	1.08	$a_{CH}^{\sigma} = -0.210$
8	C=C (C_2H_4)	1.34	$a_{CC}^{\sigma\cdot\pi} = -0.183$
9	C(sp^2)—C(sp^3)	1.53	$a_{CC}^{\sigma\cdot\pi} = 0.275$
10	C(sp^2)—H	1.08	$a_{CH}^{\sigma\cdot\pi} = 0.454$

[a] The values indicated $a_{ij}^{\sigma\cdot\pi}$ are expressed for total ($\sigma + \pi$) electronic charges, eq. [5]; a_{ij}^{σ} refers to changes in σ electrons only. The results 2, 4, and 5 are from refs. 1 and 2; 8–10, describing ethylenic carbons, are from refs. 2 and 4.

therefrom, the corresponding enthalpies of formation, ΔH_f^0 (gas, 298.15 K).

Calculation of the a_{ij} *parameters*

The appropriate expression is (1, 2)

$$[4] \quad a_{ij} = \frac{3/7}{\nu_i K_i^{\mathrm{mol}}}\left[\left(\frac{\partial E_i^{\mathrm{vs}}}{\partial N_i}\right)^0 - \frac{1}{2}\left(\frac{\partial^2 E_i^{\mathrm{vs}}}{\partial N_i^2}\right)^0 \Delta q_i\right] - \frac{3}{7} Z_j^{\mathrm{eff}} \langle r_{ij}^{-1}\rangle^0$$

where Z^{eff} are effective nuclear charges (7–9) (e.g., 4 for C), ν_i = number of atoms attached to i, and $\langle r_{ij}^{-1}\rangle^0$ is the average inverse distance between the N_i electrons of atom i and the nucleus of atom j. K_i^{mol} is $\frac{1}{2}$ for H and 0.4287 for C (1, 2, 10). The factor $\frac{3}{7}$ translates nuclear-electronic into total (potential + kinetic) energy changes (1, 2, 10, 11). The derivatives of the appropriate valence state energy of atom i, E_i^{vs}, follow from SCF-Xα calculations (Appendix I). The second-order term being negligible for hydrogen and carbon, all the a_{ij}'s used in this work can be treated as constants. The most frequently occurring values are indicated in Table 1.

With sp^2 carbons, whose charges vary at both the σ and π levels, the $a_{ij}\Delta q_i$ term becomes $a_{ij}^{\sigma}\Delta q_i^{\sigma} + a_{ij}^{\pi}\Delta q_i^{\pi}$; a_{ij} is thus the weighted average of a_{ij}^{σ} and a_{ij}^{π} (2). Taking advantage of the relationship (12) $\Delta q_i^{\sigma} = m\Delta q_i^{\pi}$, this average is (4)

$$[5] \quad a_{ij} = (m a_{ij}^{\sigma} + a_{ij}^{\pi})/(1 + m)$$

For nonsubstituted aromatic carbons, it is found that $m \simeq -0.812$ (Appendix II); substitution (e.g. with a methyl group) changes m to ~ -0.90. For ethylenic carbons, $m = -0.955$ (4, 5). Equations [4] and [5] sum up the calculation of the a_{ij}'s.

Reference bond energies, ϵ_{ij}^0

The reference bonds ϵ_1–ϵ_5 (Table 2) were described earlier (1–3). Additional, frequently occurring reference energies are conveniently deduced with the help of the function[2] (1, 2, 13)

$$[6] \quad F = -\frac{3}{7}\sum_i\sum_j Z_i^{\mathrm{eff}} q_j(\langle r_{ij}^{-1}\rangle - \langle r_{ij}^{-1}\rangle^0) - \frac{3}{7} \times \sum_i\sum_j Z_i^{\mathrm{eff}} Z_j^{\mathrm{eff}}[(R_{ij}^{-1}) - (R_{ij}^{-1})^0 - (\langle r_{ij}^{-1}\rangle - \langle r_{ij}^{-1}\rangle^0)]$$

which contains information regarding orbital shapes and internuclear distances, R_{ij}. This function is part of ΔE_a^* and nonzero if actual $\langle r_{ij}^{-1}\rangle$ and (or) R_{ij} parameters differ from those assumed in the definition of any ϵ_{ij}^0 included in $\Sigma\epsilon_{ij}^0$. (This situation arises, for example, if ethylene is constructed with ethane CH reference bonds.) In contrast, *when the* ϵ_{ij}^0*'s are properly chosen, results derived from eq. [3] show that* $F \simeq 0$ *is a valid approximation*[3] (cf. Fig. 1), hence the merits of defining suitable ϵ_{ij}^0's. This is achieved by modifying ϵ_{ij}^0's deduced for $\langle r_{ij}^{-1}\rangle^0$ and $(R_{ij}^{-1})^0$ into values corresponding to $\langle r_{ij}^{-1}\rangle$ and (R_{ij}^{-1}), as requested by eq. [6].[4] Changes in reference charges, if desired, are made with the help of eq. [1]. Thus we deduce, for example, the ethylene and benzene CH bonds from that of ethane, or CC single bonds like those in biphenyl, *cis*-stilbene, etc., from that of ethane.

While a unified new genealogy of chemical bonds surfaces with eq. [6], the pivotal question rests here with our approximate way of applying it in a possibly rough, but certainly simple, scheme satisfying chemical intuition. The underlying hypotheses and detailed numerical examples illustrating the use of eq. [6] are given in Appendix III. These hypotheses are eventually going to be put on trial in extensive comparisons with experimental results. With the set of reference bond energies indicated in Table 2, F is ~0 again, and energy calculations can be made in a straightforward manner using eq. [3].

Charge calculations

Net charges of alkane carbon atoms are conveniently deduced from the remarkably accurate relationship (1, 2, 15)

$$[7] \quad \Delta q_C = -0.148\,\delta^{C_2H_6}\,\mathrm{me}$$

where the ^{13}C nmr shift, $\delta^{C_2H_6}$ (ppm), and $\Delta q_C = q_C - q_C^0(C_2H_6)$ are expressed with reference to ethane. Similarly, for ethylenic sp^2 carbons we use (4)

$$[8] \quad \Delta q_C = 0.15\,\delta^{C_2H_4}\,\mathrm{me}$$

where the nmr shifts, $\delta^{C_2H_4}$ and $\Delta q_C = q_C - q^0{}_C(C_2H_4)$ are expressed taking ethylene as reference. Finally, for aromatic carbons we use (Appendix II)

$$[9] \quad \Delta q_C = 1.20\,\delta^{C_6H_6}\,\mathrm{me}$$

where both Δq_C and $\delta^{C_6H_6}$ are taken with reference to the benzene carbon atom. Note that eqs. [8] and [9] are for total ($\sigma + \pi$) net charges. These results serve two purposes, namely, the calculation of individual $a_{ij}\Delta q_i$ terms and that of the total net charge on all carbon atoms. The latter is obtained from a sum of

---

[2] The quantities appearing in eq. [6] are defined in terms of a suitable partitioning of the molecular electron density into atomic contributions, ρ_i, and of the equilibrium coordinates, r_i, of the nuclei, i.e.,

$$\int \frac{\rho_i(\boldsymbol{r})}{|\boldsymbol{r} - \boldsymbol{r}_i|}\,\mathrm{d}\boldsymbol{r} = N_i\langle r_i^{-1}\rangle \text{ with } \int \rho_i(\boldsymbol{r})\,\mathrm{d}\boldsymbol{r} = N_i$$

$$\int \frac{\rho_i(\boldsymbol{r})}{|\boldsymbol{r} - \boldsymbol{r}_i|}\,\mathrm{d}\boldsymbol{r} = N_j\langle r_{ij}^{-1}\rangle \text{ with } \int \rho_j(\boldsymbol{r})\,\mathrm{d}\boldsymbol{r} = N_j$$

The superscript zero indicates the corresponding expressions for the reference molecule.

[3] The first part is small because atomic net charges are small (e.g., <0.0351 e for sp^3 and ~0.007 e for ethylenic sp^2 carbons) and because small changes in electron populations are unlikely to modify their center of charge to any significant extent. The second part, in square brackets, is obviously zero for spherically symmetric electron clouds or small if the centers of electronic charge move along with the nuclei during small changes in internuclear distances.

[4] For example, eq. [6] predicts $F = -2.39$ kcal mol^{-1} for an ethylenic CH bond and -4.80 kcal mol^{-1} for a CC single bond formed by an ethylenic carbon (4, 5, 13, 14). Systematic inclusion of these results in the ϵ_{ij}^0's corresponding to these bonds takes care of F. Figure 1 includes ~50 olefins calculated in this manner.

TABLE 2. Frequently used reference bond energies[a]

Bond	i—j	Type	R_{ij} (Å)	Reference charge (me) i	j	ϵ^0_{ij}(kcal mol^{-1})
1	C—C	sp^3—sp^3	1.53	35.1	35.1	69.633
2	C=C	sp^2—sp^2	1.34	7.7	7.7	139.27
3	C—C	sp^2—sp^2	1.46	7.7	7.7	89.70
4	C┅C	Ar—Ar	1.40	14.8	14.8	114.21
5	C—H	sp^3—H	1.08	35.1	−11.7	106.806
6	C—C	Ar—Ar	1.40	14.8	14.8	91.56
7	C—C	Ar—sp^3	1.53	14.8	35.1	79.30
8	C—C	Ar—sp^2(nc)	1.49	14.8	7.7	86.89
9	C—C	Ar—sp^2(c)	1.48	14.8	7.7	90.40
10	C—C	sp^2—sp^3	1.53	7.7	35.1	77.70
11	C—H	Ar—H	1.08	14.8	−11.7	111.58
12	C—H	sp^2—H	1.08	7.7	−11.7	110.68

[a] Bond 8 is nonconjugated, 9 is conjugated, Ar = aromatic C atom, sp^2 indicates an ethylenic carbon. The following ϵ^0_{ij}'s are taken from previous work: 1, 5 (1), 2, 10, 12 (4) and 3 (5). Bonds 1, 3, and 5 were used for deducing 6–12. The reference charge selected for benzene, 14.8 me, is discussed in Appendix II.

all Δq_i's to which are added 35.1 me for each sp^3 carbon, 14.8 me for each aromatic, and 7.7 me for each ethylenic sp^2 carbon of the molecule. This gives the sum Σq_C and $\Sigma q_H = -\Sigma q_C$. The reference for hydrogen being taken in all cases at −11.7 me, it follows that

$$[10] \quad \Sigma\Delta q_H = -\Sigma q_C + 11.8\, n_H \text{ me}$$

where n_H is the number of hydrogen atoms. This concludes the derivation of the charges required in the forthcoming energy calculations.

The calculation of atomization energies, ΔE_a^*

We can now apply eq. [3]. The calculation of $\Sigma\epsilon^0_{ij}$ is straightforward, using Table 2. There is one point to be mentioned. The aromatic CC bond, ϵ_4, represents, so to speak, the average between a single and double bond as they are found in benzenoid structures: it is the CC bond of benzene. It is counted twice the number of double bonds one can write using classical Kekulé structures. The remaining CC bonds (e.g., 1 in naphthalene, 2 in anthracene, etc.) are treated as C(sp^2)—C(sp^2) single bonds—bond ϵ_6 in Table 2.

As regards the evaluation of $\Sigma_i\Sigma_j a_{ij}\Delta q_i$, first we calculate $\Sigma_j a_{ij}$ for each carbon atom, using Table 1. These sums are conveniently displayed in structure **I**. Next, we calculate the corresponding Δq_C's and form the product $\Delta q_i \Sigma_j a_{ij} = \Sigma_j a_{ij}\Delta q_i$ for each carbon, as in the example given in Table 3. The sum of these atomic terms over all carbon centers i yields the corresponding part of $\Sigma_i\Sigma_j a_{ij}\Delta q_i$. Finally, we calculate $\Sigma\Delta q_H$ and add −0.632 $\Sigma\Delta q_H$ to the previous sum. This is now $\Sigma_i\Sigma_j a_{ij}\Delta q_i$, ready for use in eq. [3].

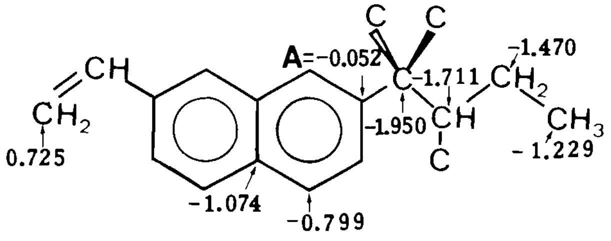

I

Sum of the a_{ij} terms for the various types of atoms, $\Sigma_j a_{ij}$, in kcal mol^{-1} me^{-1}.

TABLE 3. Calculation of $\Sigma_i\Sigma_j a_{ij}\Delta q_i$ (kcal mol^{-1}) for 2-methylnaphthalene, using the a_{ij}'s of Table 1 and eqs. [7] and [9][a]

Atom	δ	Δq	$\Sigma_j a_{ij}$	$\Sigma_j a_{ij}\Delta q_i$
1	−1.5	−1.80	−0.799	1.438
2	6.8		(−0.052)	−0.354
3	−0.45	−0.54	−0.799	0.431
4	−0.7	−0.84	−0.799	0.671
5	−0.7	−0.84	−0.799	0.671
6	−3.6	−4.32	−0.799	3.452
7	−2.7	−3.24	−0.799	2.589
8	−1.1	−1.32	−0.799	1.055
9	5.6	6.72	−1.074	−7.217
10	3.65	4.38	−1.074	−4.704
CH_3	16.35	−2.42	−1.229	2.974
$\Sigma\Delta q_H$		−61.88	−0.632	39.108

[a] The δ's are relative to benzene (1–10) and to ethane for the methyl carbon. From the Δq_c's (me), counting 14.8 me for each aromatic carbon and 35.1 me for the sp^3 reference, it is Σq_C = 178.88 and $\Sigma\Delta q_H$ = −178.88 − 10(−11.7) me. Note the contribution of C—2, −0.052 δ = −0.354 kcal mol^{-1}. The sum of all the $\Sigma_i\Sigma_j a_{ij}\Delta q_i$'s yields 40.11 kcal mol^{-1}, ready for use in eq. [3].

There is one case which is treated in a slightly different manner, with no loss in simplicity, that of an aromatic carbon attached to a non-aromatic carbon. Its contribution is −0.052 $\delta^{C_6H_6}$ kcal mol^{-1}. This carbon is taken at 14.8 me in the computation of Σq_C. The reason for this approach stems from a situation of small differences between large numbers (explained in Appendix IV) arising in the evaluation of $\Sigma_j a_{ij}$.

In closing, let us mention a simple formula for nonsubstituted aromatic hydrocarbons, taking care of $\Sigma\Delta q_H$ by charge normalization and using the a_{ij}'s of Table 1, as well as eq. [9]. It is, indeed, readily deduced that

$$\Sigma_i\Sigma_j a_{ij}\Delta q_i = -0.33\, \Sigma N_{CC}\delta^{C_6H_6} + 0.46\, \Sigma\Delta^{C_6H_6} + 0.632\,(14.8\, n_C - 11.7\, n_H)$$

where N_{CC} = number of CC bonds formed by the carbon whose

TABLE 4. Energy calculations of selected planar benzenoid hydrocarbons, using ^{13}C nmr shifts (kcal mol^{-1})[a]

Molecule	$\Sigma N_{CC}\delta$	$\Sigma\delta$	$\Sigma_i\Sigma_j a_{ij}\Delta q_i$	$\Sigma\epsilon_{ij}^0$	ΔE_a^*
Benzene	0	0	11.76	1354.74	1366.50
Naphthalene	7.2	−1.6	31.27	2127.50	2158.77
Anthracene	50.1	17.6	48.57	2900.26	2948.83
Phenanthrene	−4.5	−8.0	54.81	2900.26	2955.07
Pyrene	−30.2	−17.1	77.81	3217.84	3295.65
Benz[*a*]anthracene	17.3	−0.7	73.60	3673.02	3746.62

[a] The average deviation between these calculated atomization energies and their experimental counterparts is 0.23 kcal mol^{-1} (see Table 5). The sources of the nmr shifts are indicated at the bottom of Table 5.

nmr shift is $\delta^{C_6H_6}$, n_C = number of C atoms, and n_H = number of H atoms in the molecule. Selected numerical examples are indicated in Table 4.

Now is the proper time to look at thermochemical results in order to assess the validity of our approach toward solving eq. [3].

Results

Most of the benzenoid hydrocarbons for which both the enthalpy of formation, ΔH_f^0 (gas, 298.15), and the carbon-13 nmr spectrum are experimentally known were examined in the present work. While experimental ΔH_f^0 results are typically reported with an error of 0.3–1.0 kcal mol^{-1}, independent measurements from different laboratories often differ from one another by much more than this. Pyrene, for example, is reported by Cox and Pilcher (16) with $\Delta H_f^0(g) = 49.94 \pm 0.64$, contrasting with the result cited by Kao and Allinger (17), 51.59 kcal mol^{-1}. Whenever reasonable, critically selected data given by Cox and Pilcher (16) were used. The structures of some of the compounds investigated here are shown in Fig. 2.

In order to offer valid comparisons with theoretical results, we must first deduce "experimental" atomization energies from enthalpies of formation, zero-point and heat-content energies, ZPE + $H_T - H_0$, and from the enthalpies of formation of the atoms, $\Delta H_f^0(A)$. The latter are taken from the literature (18), namely, $\Delta H_f^0(C) = 170.89$ and $\Delta H_f^0(H) = 52.09$ kcal mol^{-1} at 298.15 K. The appropriate equation is, for nonlinear molecules,

$$[11] \quad \Delta E_a^* = \sum_i n_i\left[\Delta H_f^0(A_i) - \frac{5}{2}RT\right] + \text{ZPE} + H_T - H_0 - \Delta H_f^0$$

Vibrational energy data are scarce, however, for the molecules considered in this study. Fortunately they can be constructed to a good approximation by means of additivity rules (2), e.g., ZPE + $H_T - H_0 \simeq 33.35 + 18.213\ (n-2) - 0.343\ n_{br}$ for a mono-olefin with n carbons and n_{br} = number of branchings, or ZPE + $H_T - H_0 \simeq 55.19 + 18.213\ (n-4)\ - 0.343\ n_{br}$ kcal mol^{-1} for diolefins (5). Similar equations are also found to apply in other homologous series of compounds, e.g., alkanes and cycloalkanes, ethers, and carbonyl compounds (2). Along these lines, we use the following formula for alkyl substitution, based on the experimental ZPE + $H_T - H_0$ value (66.22 kcal mol^{-1}) deduced for benzene in the harmonic oscillator approximation (2):

$$\text{ZPE} + H_T - H_0 = 66.22 + 18.21\ n - 0.343\ n_{br}$$

where n is the number of alkyl carbon atoms. Molecules like 9,10-dihydroanthracene or 1,2,3,4-tetrahydronaphthalene were treated in similar manner. In these situations, attention must be given to a lowering of ZPE + $H_T - H_0$ by 11.5 kcal mol^{-1} accompanying the loss of a pair of hydrogen atoms and by $\sim RT/2 = 0.296$ kcal mol^{-1} for each hindered rotation in cyclic compounds (2, 19). Moreover, the condensation of two fragments involves a correction of $4RT = 2.37$ kcal mol^{-1} because this term is included in the $H_T - H_0$ part of each molecule used as fragment and should not be counted twice in the final product. For example, the ZPE + $H_T - H_0$ value of 9,10-dihydroanthracene is obtained from dimethylbenzene ($66.22 + 2 \times 18.21$) and benzene, less 2×11.5, less $4RT$, and less $4RT/2$ kcal mol^{-1}. This type of estimate usually carries an uncertainty not exceeding 0.2 kcal mol^{-1}. Styrene, for example, can be constructed from benzene and ethylene to give ZPE + $H_T - H_0 = 66.22 + 33.35 - 11.5 - 4RT = 85.70$ kcal mol^{-1}.

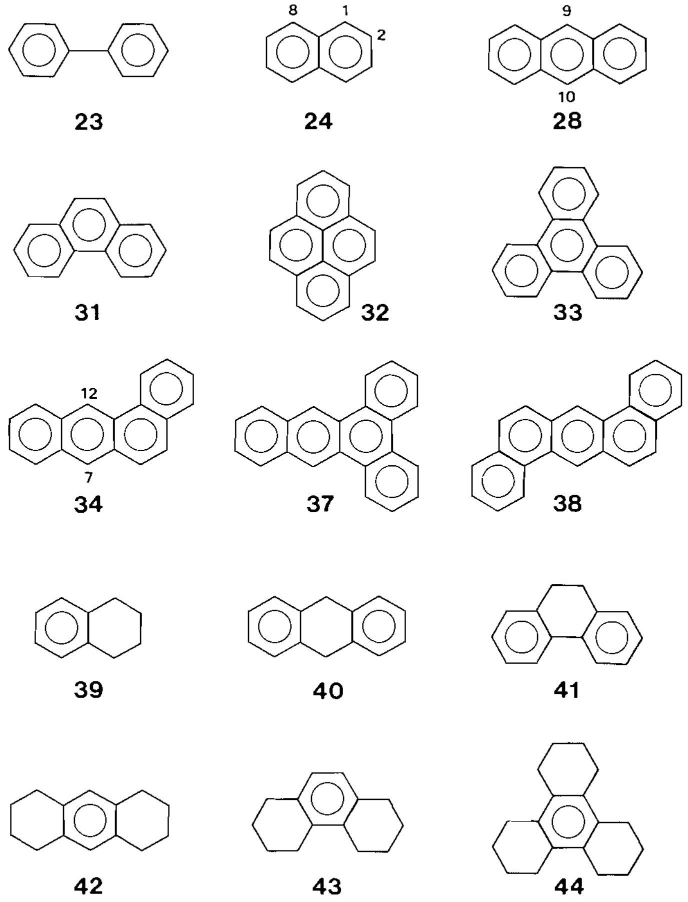

FIG. 2. A selection of molecules examined in this work. The numbering corresponds to that indicated in Table 5.

TABLE 5. Calculated and experimental energies of benzenoid hydrocarbons, kcal mol^{-1} [a]

Molecule	ΔH_f^0	ZPE + $H_T - H_0$	$\Sigma\epsilon_{ij}^0$	$\Sigma_i\Sigma_j a_{ij}\Delta q_i$	ΔE_a^*	
					Calcd.	Exptl.
1 Benzene	19.81 ± 0.13	66.22	1354.74	11.76	1366.5	1366.5
2 Toluene	11.99 ± 0.10	84.43	1642.88	20.52	1663.4	1663.2
3 1,2-Dimethylbenzene	4.56 ± 0.26	102.64	1931.02	28.78	1959.8	1959.4
4 1,3-Dimethylbenzene	4.14 ± 0.18	102.64	1931.02	29.12	1960.1	1959.9
5 1,4-Dimethylbenzene	4.31 ± 0.24	102.64	1931.02	28.38	1959.3	1959.7
6 1,2,3-Trimethylbenzene	−2.26 ± 0.29	120.85	2219.15	37.26	2256.4	2255.1
7 1,2,4-Trimethylbenzene	−3.31 ± 0.26	120.85	2219.15	36.55	2255.7	2256.2
8 1,3,5-Trimethylbenzene	−3.81 ± 0.33	120.85	2219.15	37.47	2256.6	2256.6
9 1,2,3,4-Tetramethylbenzene	−10.02	139.06	2507.29	45.20	2552.5	2551.7
10 1,2,3,5-Tetramethylbenzene	−10.71	139.06	2507.29	44.80	2552.1	2552.4
11 1,2,4,5-Tetramethylbenzene	−10.82	139.06	2507.29	44.08	2551.4	2552.5
12 Pentamethylbenzene	−17.80	157.27	2795.43	52.46	2847.9	2848.3
13 Hexamethylbenzene	−25.26	175.48	3083.57	60.99	3144.6	3144.6
14 Ethylbenzene	7.15 ± 0.19	102.64	1926.12	30.55	1956.7	1956.9
15 *n*-Propylbenzene	1.89 ± 0.19	120.85	2209.37	40.97	2250.3	2250.9
16 Isopropylbenzene	0.96 ± 0.26	120.50	2209.37	42.14	2251.5	2251.5
17 *sec*-Butylbenzene	−4.15 ± 0.31	138.71	2492.61	52.37	2545.0	2545.5
18 *tert*-Butylbenzene	−5.40 ± 0.31	138.71	2492.61	54.84	2547.4	2546.7
19 1,2-Diphenylethane	32.4 ± 0.3	155.0	3141.78	61.18	3203.0	3202.9
20 Styrene	35.30 ± 0.25	85.80	1804.40	7.12	1811.5	1810.7
21 *cis*-Stilbene	60.31 ± 0.42	138.05	3020.73	36.05	3056.8	3056.8
22 *trans*-Stilbene	52.5	138.05	3027.75	36.20	3064.0	3064.6
23 Biphenyl	43.53 ± 0.60	116.91	2575.00	37.83	2612.8	2612.4
24 Naphthalene	36.25 ± 0.45	94.90	2126.30	31.27	2157.7	2157.6
25 1-Methylnaphthalene	27.93 ± 0.64	113.11	2414.44	40.88	2455.3	2454.8
26 2-Methylnaphthalene	27.75 ± 0.62	113.11	2414.44	40.11	2454.6	2454.9
27 1,8-Dimethylnaphthalene	See text	131.32	2698.97	46.01	2745.0	2745.0
28 Anthracene	55.2 ± 1.1	123.7	2897.86	48.57	2946.4	2946.3
29 9-Methylanthracene	(42.1)	141.8	3186.00	62.09	3248.1	
30 9,10-Dimethylanthracene	(31.6)	160.0	3474.14	73.34	3547.5	
31 Phenanthrene	49.5 ± 1.1	123.7	2897.86	54.81	2952.7	2952.0
32 Pyrene	53.94 ± 0.31	133.05	3217.84	77.81	3295.7	3295.7
33 Triphenylene	61.9 ± 1.1	152.3	3660.09	86.36	3746.5	3747.1
34 Benz[*a*]anthracene	65.97	152.3	3669.42	73.60	3743.0	3743.0
35 7-Methylbenz[*a*]anthracene	(56.2)	170.5	3957.56	84.06	4041.6	
36 7,12-Dimethylbenz[*a*]anthracene	66.4 ± 1.1	188.7	4245.70	90.31	4336.0	4320.2
37 Dibenz[*a,c*]anthracene	(77.2)	181.0	4440.98	98.36	4539.3	(4540.5)
38 Dibenz[*a,h*]anthracene	(79.6)	181.0	4440.98	95.90	4536.9	(4538.0)
39 1,2,3,4-Tetrahydronaphthalene	7.3 ± 1.3	126.1	2353.53	66.67	2420.2	2420.2
40 9,10-Dihydroanthracene	38.2 ± 1.1	142.3	3007.58	75.17	3082.8	3083.1
41 9,10-Dihydrophenanthrene	(37.8)	142.3	3007.82	75.68	3083.5	
42 (1–8)-Octahydroanthracene	(−4.3)	185.9	3352.31	120.58	3472.9	
43 (1–8)-Octahydrophenanthrene	(−4.9)	185.9	3352.31	121.17	3473.5	
44 (1–12)-Dodecahydrotriphenylene	(−16.4)	245.8	4351.10	175.10	4526.2	

[a] The experimental ΔH_f^0 results for **1–8**, **14–21**, **23**, **28**, **31**, **33**, **36**, and **40** are "selected values" reported in ref. 16. The results for **9–13** are given in ref. 24, that of **22** in ref. 25, and those of **24–26** in ref. 26. The value indicated for **32** is taken from ref. 27, **34** is reported in ref. 17, and **39** is taken from ref. 28. The ZPE + $H_T - H_0$ result given for **31** was deduced from a vibrational analysis described in ref. 29, in the harmonic oscillator approximation. The carbon-13 nmr spectra are from ref. 30 (**2–13**), ref. 31 (**14–19**), and from ref. 32 (**20**, **23**, **39–44**); **21** and **22** are from ref. 33; **24**, **31**, **32** from ref. 34; and **28** is from ref. 35; **25**, **26** are given in ref. 36; **27** is from ref. 37; and **29**, **30**, **34–38** are from ref. 38; **33** is described in ref. 39. In order to minimize possible solvent effects, whenever possible measurements made in benzene were selected.

From the vibrational spectrum of styrene (20), on the other hand, we find in the harmonic oscillator approximation that ZPE = 80.96 and $H_T - H_0 = 4.84$, for a total of 85.80 kcal mol^{-1}. Similarly, using ZPE + $H_T - H_0$ = 88.82 + 5.08 = 94.90 kcal mol^{-1} for naphthalene, deduced from its vibrational spectrum (21), we add to it the difference, 28.68 kcal mol^{-1}, between naphthalene and benzene, thus obtaining an estimate of 123.6 kcal mol^{-1} for anthracene. The same procedure is used for the higher homologues as well. Finally, using the fundamental frequencies of pyrene (22), we obtain (in the harmonic oscillator approximation) ZPE = 125.94, $H_T - H_0 = 7.11$, for a total of 133.05 kcal mol^{-1}.

While, of course, additional spectroscopic information would be welcome, we feel that the uncertainties affecting present estimates of ZPE + $H_T - H_0$ energies should not be blamed for possible discrepancies between calculated and observed ΔE_a^* (or ΔH_f^0) energies. With this in mind, we can now proceed with comparisons involving experimental enthalpies of formation (Table 5). In the absence of experimental results, predicted ΔH_f^0 values are indicated in parentheses. Two ΔE_a^* results listed in the column reporting "experimental values" are in parentheses: these are theoretical results offered for comparison, deduced from enthalpies of formation calculated by Dewar and de Llano (23).

Discussion

The average deviation between calculated and experimental energies is 0.36 kcal mol^{-1} for a collection of 35 benzenoid compounds. This result does not include 7,12-dimethylbenz[*a*]anthracene: the discrepancy of ~16 kcal mol^{-1} between theory and experiment is in all likelihood due in part to an error in the latter. Although certainly real, steric interactions involving the methyl group in position 12 are probably not so severe as to cause a destabilization exceeding that found in 1,8-dimethylnaphthalene and 4,5-dimethylphenanthrene—molecules which are discussed further below.

At this stage it seems safe to conclude that the agreement between theory and experiment supports the general ideas underlying our energy analysis. On the other hand, the quality of this agreement should not be used to hide the limitations of our approach. These are best revealed by the following examples. *Trans*-stilbene was treated as a planar system and the C(sp^2)—Ph bonds were accordingly derived on the basis of a conjugated sp^2—sp^2 single bond (Appendix III, example 6). While the molecular structure of *trans*-stilbene appears to be approximately planar in the solid state (40), its gas phase structure is found to be nonplanar (41). However, the potential curve for energy vs. the dihedral angle is very shallow and the calculated energy barrier corresponding to the C_i conformation is only about 0.5 kcal mol^{-1} (17). Both these results and our calculation suggest that in *trans*-stilbene there is no great energy difference between conjugation and hyperconjugative stabilization of the sp^2—sp^2 single bond[5] but it is also clear that in this particular situation it could not be assumed *a priori* that our treatment would lead to a valid result, as it did. The case of *cis*-stilbene is clear-cut. Electron diffraction data (43) point to a C_2 symmetry in the gas phase and a structure that may be described as having a propeller-like conformation with phenyl groups rotated ca. 43° about the C—Ph bonds. The latter were thus treated as nonconjugated bonds: $\epsilon_8 = 86.89$ kcal mol^{-1} was deduced for $R_{CC} = 1.49$ Å, which is the experimental bond length (43). Similarly, the gas phase value (44) for the torsional angle about the central bond of biphenyl, 41.6°, and its bond length, $R = 1.49$ Å (17, 45), suggest that the central bond should be treated like a nonconjugated CC single bond, thus giving $\epsilon_{CC} = 88.68$ kcal mol^{-1}. Finally, the same situation arises with triphenylene (**33**) which is significantly nonplanar (17, 46). The bonds joining the "external" rings to one another were thus calculated at $\epsilon_{CC} = 88.45$ kcal mol^{-1} for $R = 1.46$ Å, following the approach used for biphenyl. It is clear that some advance knowledge is necessary in our calculations, namely, as regards planarity (or lack of it) of the benzenoid skeleton.

As an additional example, consider 4,5-dimethylphenanthrene. Using the ^{13}C nmr spectrum measured by Stothers *et al.* (47), we deduce $\Delta H_f^0 = 36.8$ kcal mol^{-1} assuming planarity. Closely neighboring methyl groups which are separated by five bonds in the molecular skeleton, however, result in chiral nonplanar conformations (48). Modeling, where appropriate, the CC bonds on those described for biphenyl and *cis*-stilbene, we predict $\Delta H_f^0 = 47.8$ for the nonplanar form, in acceptable accord with the reported value (16), 46.26 ± 1.46 kcal mol^{-1}, a result which is self-explanatory. Equally instructive examples are offered by dimethylnaphthalene isomers. With the substituents in the 1,8 position, our calculation yields $\Delta E_a^* = 2748.6$ kcal mol^{-1} for the planar form, in error with respect to its experimental counterpart,[6] 2745.0 kcal mol^{-1}. The thermochemical stability is overestimated by ~3.6 kcal mol^{-1}, thus suggesting a possible loss of conjugation in this molecule which, as a matter of fact, is known to suffer considerable distortion from the normal naphthalene geometry (50). Indeed, a calculation following the lines described above for biphenyl and nonplanar 4,5-dimethylphenanthrene agrees with experiment. In contrast, 2,6-dimethylnaphthalene can safely be assumed to retain the planar geometry of naphthalene. The result deduced for this form, $\Delta E_a^* = 2751.3$, agrees well with the experimental value,[6] 2751.0 kcal mol^{-1}. These examples illustrate possible applications of energy analyses based on ^{13}C spectra in problems regarding the origin of molecular stability, namely, as regards partial suppression of conjugation accompanying deformations of a benzenoid skeleton.

These examples are also there to remind us that our theory differs in its nature from variational calculations and thus lacks the flexibility of the latter, capable of predicting geometries as well as energies. Indeed, our approach applies only to molecules at equilibrium; in turn, it illustrates efficiently the role of local charges, namely, the way they affect chemical bonds. It is certainly gratifying to recognize how intimately bonds of different types are related to one another, e.g., the CH bonds of ethane, ethylene, and benzene or the CC single bonds of ethane, toluene, *cis*-stilbene, and biphenyl. Minor uncertainties plagueing numerical applications should not obscure the fundamental simplicity of the arguments describing bond energies in terms of local charges. The general concepts developed here, capable of describing chemical bonds in a unifying picture encompassing well-diversified situations, are more relevant, in our opinion, than the precision of the calculations supporting these views. At the present level, residual uncertainties resulting from occasional computational approximations are of the order of those affecting experimental results and are not of the sort that could threaten the essence of the basic ideas underlying our description of molecular energies.

While, of course, our approach does not have the potential of true density functional theory based on the Hohenberg–Kohn theorem (51), it offers at least a conceptually related, simple, and instructive solution when both local charges and nuclear positions are given for a ground-state molecule at equilibrium. At this relatively modest level, it becomes clear that the theory of chemistry and of the chemical bond are in essence a theory of electron density, a fact which can now be described in simple terms for a great variety of organic molecules.

Acknowledgements

The financial support given by the Natural Sciences and Engineering Research Council of Canada and the cooperation of the Centre de Calcul de l'Université de Montréal are gratefully acknowledged.

---

[5] Related analyses regarding the stabilization of sp^2—sp^2 single bonds are offered in ref. 42.

[6] These results were deduced from eq. [11] using thermochemical data at 350–370 K given in ref. 49.

1. S. Fliszár. J. Am. Chem. Soc. **102**, 6946 (1980).
2. S. Fliszár. Charge distributions and chemical effects. Springer Verlag, New York. 1983.
3. S. Fliszár. Int. J. Quantum Chem. **26**, 743 (1984).
4. M.-T. Béraldin and S. Fliszár. Can. J. Chem. **61**, 197 (1983).
5. S. Fliszár and G. Cardinal. Can. J. Chem. **62**, 2748 (1984).
6. S. Fliszár and M.-T. Béraldin. Can. J. Chem. **60**, 792 (1982).
7. P. Politzer and R. G. Parr. J. Chem. Phys. **61**, 4258 (1974); **64**, 4634 (1976).
8. S. Fliszár and H. Henry. J. Chem. Phys. **67**, 2345 (1977); S. Fliszár and D. Salahub. J. Chem. Phys. **69**, 3321 (1978); R. J. Boyd. J. Chem. Phys. **66**, 356 (1977).
9. S. Fliszár. J. Chem. Phys. **79**, 3874 (1983).
10. S. Fliszár, M. Foucrault, M.-T. Béraldin, and J. Bridet. Can. J. Chem. **59**, 1074 (1981).
11. P. Politzer. J. Chem. Phys. **64**, 4239 (1976); S. Fliszár and M.-T. Béraldin. J. Chem. Phys. **72**, 1013 (1980); T. Anno. J. Chem. Phys. **72**, 782 (1980); P. Politzer. J. Chem. Phys. **70**, 1067 (1979).
12. S. Fliszár, G. Cardinal, and M.-T. Béraldin. J. Am. Chem. Soc. **104**, 5287 (1982); W. J. Hehre, R. W. Taft, and R. D. Topsom. Progr. Phys. Org. Chem. **12**, 159 (1976).
13. S. Fliszár, G. Del Re, and M. Comeau. Can. J. Chem. **63**, 3551 (1985).
14. M.-T. Béraldin. Ph.D. Thesis, Université de Montréal (1985).
15. S. Fliszár, A. Goursot, and H. Dugas. J. Am. Chem. Soc. **96**, 4358 (1974).
16. J. D. Cox and G. Pilcher. Thermochemistry of organic and organometallic compounds. Academic Press, London, New York. 1970.
17. J. Kao and N. L. Allinger. J. Am. Chem. Soc. **99**, 975 (1977).
18. D. R. Stull and G. C. Sinke. Adv. Chem. Ser. **18**, (1956).
19. S. Fliszár and J.-L. Cantara. Can. J. Chem. **59**, 1381 (1981).
20. A. Marchand and J.-P. Quintard. Spectrochim. Acta Part A, **36**, 941 (1980).
21. S. S. Mitra and H. J. Bernstein. Can. J. Chem. **37**, 553 (1959).
22. A. Bree, R. A. Kydd, T. N. Misra, and V. V. B. Vilkos. Spectrochim. Acta. Part A, **27**, 2315 (1971).
23. M. J. S. Dewar and C. de Llano. J. Am. Chem. Soc. **91**, 789 (1969).
24. S. H. Hastings and D. E. Nicholson. J. Phys. Chem. **61**, 730 (1957).
25. S. Marantz and G. T. Armstrong. J. Chem. Eng. Data, **13**, 118, 455 (1968).
26. D. M. Speros and F. D. Rossini. J. Phys. Chem. **64**, 1723 (1960).
27. N. K. Smith, R. C. Stewart Jr., A. G. Osborn, and D. W. Scott. J. Chem. Thermodyn. **12**, 919 (1980).
28. W. D. Good and S. H. Lee. J. Chem. Thermodyn. **8**, 643 (1976).
29. S. J. Cyvin, G. Neerland, J. Brunvoll, and N. B. Cyvin. Spectrosc. Lett. **14**, 37 (1981).
30. W. R. Woolfenden and D. M. Grant. J. Am. Chem. Soc. **88**, 1496 (1966).
31. Sadtler standard carbon-13 nmr spectra. Sadtler Research Laboratories, Inc., Philadelphia.
32. J. B. Stothers. Carbon-13 nmr spectroscopy. Academic Press, New York, NY. 1972.
33. T. W. Proulx and W. B. Smith. J. Magn. Reson. **23**, 447 (1976).
34. T. D. Alger, D. M. Grant, and E. G. Paul. J. Am. Chem. Soc. **88**, 5397 (1966).
35. R. J. Pugmire, D. M. Grant, M. J. Robins, and R. K. Robins. J. Am. Chem. Soc. **91**, 6381 (1969).
36. D. Doddrell and P. R. Wells. J. Chem. Soc. Perkin Trans. 2, 1333 (1973).
37. A. J. Jones, T. D. Alger, D. M. Grant, and W. M. Litchmann. J. Am. Chem. Soc. **92**, 2386 (1970).
38. R. S. Ozubko, G. W. Buchanan, and I. C. P. Smith. Can. J. Chem. **52**, 2493 (1974).
39. A. J. Jones and D. M. Grant. Chem. Commun. 1670 (1968).
40. C. J. Finder, M. G. Newton, and N. L. Allinger. Acta Crystallogr. Sect. B, **30**, 411 (1974); A. Koekstra, P. Meertens, and A. Vos. Acta Crystallogr. Sect. B, **31**, 2813 (1975).
41. M. Traetteberg, E. B. Frantsen, F. C. Mijhoff, and A. Koekstra. J. Mol. Struct. **26**, 57 (1975).
42. H. Kollmar. J. Am. Chem. Soc. **101**, 4832 (1979); J. P. Daudey, G. Trinquier, J. C. Barthelat, and J. P. Malrieu. Tetrahedron, **36**, 3399 (1980).
43. M. Traetteberg and E. B. Frantsen. J. Mol. Struct. **26**, 69 (1975).
44. O. Bastiansen and M. Traetteberg. Tetrahedron, **17**, 147 (1962).
45. A. Almenningen and O. Bastiansen. Skr. K. Nor. Vidensk. Selsk. **4**, 1 (1958).
46. P. R. Pinnock, C. A. Taylor, and H. Lipson. Acta Crystallogr. **9**, 173 (1956); F. R. Ahmed and J. Trotter. Acta Crystallogr. **16**, 503 (1963).
47. J. B. Stothers, C. T. Tan, and N. K. Wilson. Org. Magn. Reson. **9**, 408 (1977).
48. R. Munday and I. O. Sutherland. J. Chem. Soc. B, 80 (1968).
49. H. L. Finke, J. F. Messerly, S. H. Lee, A. G. Osborn, and D. R. Douslin. J. Chem. Thermodyn. **9**, 937 (1977).
50. W. D. Good. J. Chem. Thermodyn. **5**, 715 (1973).
51. P. Hoehenberg and W. Kohn. Phys. Rev. Sect. B, **136**B, 864 (1964).
52. B. I. Dunlap, J. W. D. Connolly, and J. R. Sabin. J. Chem. Phys., **71**, 4993 (1979); H. Sambe and R. H. Felton. J. Chem. Phys. **62**, 1122 (1975).
53. S. Huzinaga. J. Chem. Phys. **42**, 1293 (1965).
54. T. H. Dunning. J. Chem. Phys. **55**, 716 (1970).
55. F. Herman and S. Skillman. Atomic structure calculations. Prentice–Hall, Englewood Cliffs, NJ. 1963.
56. A. H. Stroud. Approximate calculation of multiple integrals. Prentice–Hall, Englewood Cliffs, NJ. 1971.
57. J. C. Slater. The self consistent field for molecules and solids. McGraw–Hill, New York, NY. 1974; K. H. Johnson. Adv. Quantum Chem. **7**, 143 (1973).
58. G. Cardinal, N. A. Baykara, and S. Fliszár. To be published.
59. K. Schwarz. Phys. Rev. B, **5**, 2466 (1972).
60. W. J. Hehre, R. F. Stewart, and J. A. Pople. J. Chem. Phys. **51**, 2657 (1969).
61. R. S. Mulliken. J. Chem. Phys. **23**, 1833 (1955); **23**, 1841 (1955); **23**, 2338 (1955); **23**, 2343 (1955).
62. K. Tamagawa, T. Iijma, and M. Kimura. J. Mol. Struct. **30**, 243 (1976).
63. S. N. Ketkar and M. Finki. J. Mol. Struct. **77**, 139 (1981).
64. A. Almenningen, O. Bastiansen, and F. Dyvik. Acta Crystallogr. **14**, 1056 (1961).
65. M. I. Kay, Y. Okaya, and D. E. Cox. Acta Crystallogr. Sect B, **27**, 26 (1971).
66. M. Said, D. Maynau, J.-P. Malrieu, and M.-A. Garcia Bach. J. Am. Chem. Soc. **106**, 571 (1984).

Appendix I

The $\partial E/\partial N$ derivatives were obtained from LCAO-Xα calculations by means of the programs developed by Dunlap *et al.* (52). Huzinaga's ($9s5p$) basis (53) was used for ground-state carbon. Hydrogen was described by a ($5s$) basis obtained from Dunning's ($3s$) basis set (54). In the LCAO-Xα method it is necessary to fit the charge density and the exchange potentials to sets of auxiliary Hermite gaussian functions. The Xα exchange potentials were fitted to the auxiliary functions following the criterion given by Dunlap *et al.* (52), i.e.,

$$\int \rho\widetilde{(\rho^{1/3})}\,\mathrm{d}\tau = \int \widetilde{(\rho^{1/3})}^{4}\,\mathrm{d}\tau$$

TABLE A1. $(\partial E/\partial N)_\pi$ and $(\partial E/\partial N)_\sigma$ values (au) for use in eq. [4][a]

Molecule	Orbital	$(\partial E/\partial N)$, au		
		α_{HF}	$\alpha_{exptl.}$	Selected
Benzene	π	−0.259	−0.264	−0.262
	σ	−0.372	−0.379	−0.375
Ethylene	π	−0.244	−0.248	−0.246
	σ	−0.373	−0.378	−0.375

[a] Additional results are reported in refs. 1 and 2.

where the tilde represents a fitted quantity. The sampling points for the exchange potentials were determined by taking each tenth point of the Herman–Skillman radial mesh (55) and an angular mesh consisting of the twelve vertices of a regular icosahedron (56). The auxiliary functions were selected as suggested by Dunlap *et al.* (52) for first-row diatomics: *s*-type functions were employed for the charge density fit, having orbital exponents twice those of the corresponding *s*-type gaussians used for the orbital basis. Five orbital exponents (5.0, 2.0, 0.6, 0.3, 0.1) were used for *p*-type functions. The exponents of every other *p* function used in the orbital basis were doubled to construct *d*-type Hermite gaussians for fitting the Coulomb potential. Bond-centered auxiliary *s* functions were also used, as suggested by Dunlap *et al.* (52). For the fit to the exchange potential, orbital exponents were taken at one-third of those of the corresponding charge density auxiliaries.

In LCAO-Xα calculations of heteronuclear systems one meets with the problem of choosing a single α value for the whole system because, contrasting with the Scattered Wave Method (57), the possibility of assigning different α values to different regions of space no longer exists. The general attitude has been to use the Kohn–Sham value of 2/3 or 0.7 in such situations. For a significant collection of organic molecules, on the other hand, we have found (58) that experimental atomization energies are well reproduced with an α value taken as an average of α_{ij}'s defined for the individual bonds, i.e.,

$$\alpha_{ij} = 1/2\,(\alpha_A + \alpha_B)$$

where (i, j) is a bond between centres A and B. The individual α_A's can be chosen following Schwarz (59), from a fit with Hartree–Fock values, or, else, from a fit with experimental energies of ground-state atoms (58). Selection of the latter α_A's yields atomization energies that are closer to their experimental counterparts (within a few kcal mol^{-1}) than the corresponding results deduced from the α_{HF} values given by Schwarz (59). The results are indicated in Table A1. The last column reports the $(\partial E/\partial N)$ values used in applications of eq. [4].

Appendix II

STO-3G charge analyses, following Pople's recipe (60) and Mulliken's scheme (61), are reported in Table A2, as well as the pertinent ^{13}C nmr shifts. Taking the σ–π separation, $\Delta q = \Delta q^\sigma + \Delta q^\pi$, into account as well as the relationships $\Delta q^\sigma = m\Delta q^\pi$, $\delta = c^\sigma\Delta q^\sigma + c^\pi\Delta q^\pi$ and $(d\delta/dq^\pi) = 157$ ppm/e (2, 12), we deduce $\delta = 0.835\,\Delta q + 178.66$ (ppm from TMS) and, hence, $\Delta q = 1.2\,\delta$ and $m = -0.812$. These results are admittedly crude. Extensive numerical analyses, however, such as those reported in Table 4, gave no reason for revision.

TABLE A2. Atomic charges (me) and ^{13}C nmr shifts (ppm from TMS) of selected benzenoid hydrocarbons[a]

Molecule	Atom	Net charge	δ
Benzene		−60.1	128.5
Naphthalene	C—1	−60.1	128.3
	C—2	−62.9	126.1
Anthracene	C—1	−57.9	130.3
	C—2	−62.6	125.7
	C—9	−56.0	132.8
Phenanthrene	C—1	−59.1	129.1
	C—2	−63.0	126.9
	C—3	−62.2	126.9
	C—4	−63.1	123.2
	C—9	−62.6	127.5

[a] Geometries were taken from electron diffraction studies of benzene (62), naphthalene (63), and anthracene (64) and from a neutron diffraction study of phenanthrene (65). The shift vs. charge correlation is generally acceptable. Atom C-4 of phenanthrene exhibits the largest deviation. The difference between calculated and experimental energies of phenanthrene is 0.76, using the shift value, and −0.34 kcal mol^{-1} using the charge result, while the reported experimental uncertainty is ±1.1 kcal mol^{-1}, a situation frustrating dedication to accuracy.

Mulliken's analysis involves a half-and-half partitioning of overlap populations. While charges of like C atoms (i.e., atoms forming the same type and number of bonds) are valid in comparisons involving them, lifting the constraint of halving overlap terms between dissimilar atoms becomes a must in realistic evaluations of absolute atomic charges (1, 2, 15). For benzene, we are presently unable to lift this constraint: hence the following approaches toward an estimate for the carbon net charge of benzene.

(*i*) The ^{13}C nmr shift of the methyl carbon in toluene, δ 21.3 ppm from TMS (32), gives $q_C = 32.77$ me, from eq. [7]. Using the correlation between methyl-C and methyl-H net charges (2), the latter are estimated at −12.38 me in toluene. The toluene CH$_3$ group is, in this approximation, 4.37 me negative. On the other hand, H replacing CH$_3$ (under otherwise identical conditions) is 9.05 me more negative than the latter (2). In this estimate, the benzene hydrogen should be negative by 13.4 me and, hence, $q_C(C_6H_6) \simeq 13.4$ me. This, of course, is a rough estimate. Now we look at an entirely different approach.

(*ii*) Applying eq. [2] to the benzene CH bond with ϵ^0_{11}, a_5, a_7, and $q^B_C = -q^B_H$ gives $\epsilon_{CH} = 107.29 + 0.422\, q^B_C$ kcal mol^{-1}, where the benzene carbon net charge, q^B_C, is now left as an unknown. Six of these CH bonds plus six CC bonds add up to give $\Delta E^*_a = 1366.5$ kcal mol^{-1}. Estimates of the CC bond energy based on SCF potentials at the nuclei (1–3) indicate that ϵ_{CC} is 1.62–1.65 times the CC bond energy of ethane, $\epsilon^0_1 = 69.633$ kcal mol^{-1}. With the ratio 1.62 there results $q^B_C = 18.1$ me; for 1.65 it is $q^B_C = 13.2$ me. Extensive numerical analyses involving all the experimental data included in Table 5 suggest that the ratio ~1.64 (giving ϵ_4) with $q^B_C = 14.8$ me represents a valid estimate. In this analysis, the uncertainty about q^B_C is unlikely to exceed 2 me. Finally, current work on graphite (to be published) shows that the uncertainty about $q^B_C = 14.8$ me is probably less than 1 me.

Appendix III

Approximate but valid estimates of eq. [6] can be obtained in a simple way. They are rooted in the following hypotheses (13). For CC and CH bonds involving sp^3 carbons, $\langle r_{ij}^{-1}\rangle$ is adequately approximated by the inverse of the appropriate internuclear distance (1), a simplifying hypothesis that locates the centers of σ charges at their respective nuclear positions. Similarly, the charge centroids of aromatic carbons are taken at their nuclear positions. The situation differs with ethylenic sp^2 carbons because their overlapping $2p$ electrons forming a π bond shift their respective charge centroids inwards (4, 5, 13, 14). A simple recipe for single bonds formed by an ethylenic carbon j is as follows. (*i*) The centroid of the $(N_j - 1)$ σ electrons of ethylene (taken as reference) is located at its nuclear position. (*ii*) The "effective" distance of a bonded nucleus i (C or H) from the $2p$ electron of j is 0.02 Å larger than R_{ij}. (*iii*) Our estimate of the average inverse distance between the N_j electrons of the sp^2 carbon and nucleus i is thus

$$\langle r_{ij}^{-1}\rangle \simeq 0.529\,[(N_j - 1)R_{ij}^{-1} + (R_{ij} + 0.02)^{-1}]/N_j \,\text{au}$$

ready for use in eq. [6]. This recipe, offered as a convenient replacement for equivalent but involved SCF analyses[7] of charge centroids (13), has proven accurate. Indeed, for a collection of ~50 olefins calculated in this approximation, the average deviation between theoretical and experimental atomization energies is ~0.25 kcal mol^{-1} (4, 5). Note that these considerations do not concern the benzenoid structures themselves, but only the ethylenic parts in molecules like styrene, stilbene, etc., reported here for the sake of completeness.

The numerical examples worked out below illustrate the use of eqs. [2] and [6] in the derivation of suitable reference bond energies, ϵ_{ij}^0. The conversion factors 1 bohr = 0.529 Å and 1 hartree = 627.51 kcal mol^{-1} were used. All a_{ij}'s are expressed in kcal mol^{-1} me^{-1} units and the energies in kcal mol^{-1}. The numbering of the a_{ij} and ϵ_{ij}^0 parameters is that indicated in Tables 1 and 2. The reference carbon net charges are (in 10^{-3} e units) 35.1 (C_2H_6), 7.7 (C_2H_4) and 14.8 (C_6H_6).

Example 1. Let us first apply the recipe given for $\langle r_{ij}^{-1}\rangle$ when j is an ethylenic C atom, with $N_i = 3.9923$ e. For a C_i—C_i single bond ($R = R^0 = 1.53$ Å) we find $\langle r_{ij}^{-1}\rangle = 0.34463$ au and $F = -4.80$ kcal mol^{-1}. For a CH bond ($R \doteq R^0 = 1.08$ A) we find $\langle r_{ij}^{-1}\rangle = 0.48758$ au and $F = -2.39$ kcal mol^{-1}. These F values are incorporated in the new ϵ_{ij}^0's describing CC and CH bonds formed by ethylenic sp^2 carbons, as shown below.

Example 2. Starting with the ethane CC bond, ϵ_1^0, we construct the $C_j(sp^2)$—$C_i(sp^3)$ bond, ϵ_{10}, with $R_{CC} = 1.53$ Å, $q_j = 7.7$, and $q_i = 35.1$ me. The change from 35.1 to 7.7 me (using the average of $a_2 = -0.488$ and $\alpha_6 = -0.450$) modifies ϵ_1^0 to give $\epsilon_{CC} = 82.49$; adding $F = -4.80$, one obtains 77.7 for ϵ_{10}. Similarly, starting now with the ethane CH bond, ϵ_5, the change from 35.1 to 7.7 me at the C atom (using the average of $a_4 = -0.247$ and $a_7 = -0.210$ in eq. [2] leads to $\epsilon_{CH} = 113.07$; with $F = -2.39$, it follows that $\epsilon_{12} = 110.68$ for the $C(sp^2)$—H reference bond (13).

Example 3. For aromatic carbons, we keep the centers of charge as in the bond described above, $\epsilon_{CC} = 82.49$, hence $F = 0$. To obtain ϵ_7, we start with this result and modify the charge from 7.7 to 14.8 me, using $a_6 = -0.450$. Thus, $\epsilon_7 = 82.49 - 0.450\,(14.8–7.7) = 79.30$. Similarly, the 113.07 result quoted above leads to $\epsilon_{11} = 113.07 - 0.210\,(14.8–7.7) = 111.58$.

Example 4. ϵ_7 was obtained from ϵ_1 by replacing one CH_3 of ethane by phenyl. The nonconjugated central bond of biphenyl is deduced from $2(\epsilon_7 - \epsilon_1) + \epsilon_1$ and $F = -0.29$, which reduces R from 1.53 to 1.49 Å with $q_C = 14.8$ me. The reference ϵ_8 (for a CC single bond, as in *cis*-stilbene) is deduced from ϵ_7 ($R = 1.53$ Å), which is reduced to 1.49 Å with $F = -5.40$. Using the average of a_2 and $a_{CC}^{\sigma} = -0.460$ (for 1.53 and 1.49 Å, respectively) for evaluating the change from 35.1 to 7.7 me at the sp^2 carbon, we find $\epsilon_8 = 79.30 - 5.40 + 12.99 = 86.89$.

Example 5. Here we begin with $\epsilon_3 = 89.70$ (a conjugated CC single bond formed by sp^2 carbons, as in 1,3-butadiene) (5) at its equilibrium distance, ~1.48 Å, and construct a C(Ar)—C(Ar) single bond modelled on benzene, with $R = 1.397$ Å. For $q_i = q_j = 7.7$ me, $F = 9.90$. Setting the charges at 14.8 me, using $a_{CC}^{\sigma} = -0.486$, reduces ϵ_{CC} by 6.90. The final result, 92.70, is in moderate agreement with its counterpart, 91.56, obtained from a numerical analysis of experimental data. Contrasting with the previous examples, this case illustrates a limitation of our simple evaluation of $\langle r_{ij}^{-1}\rangle$ for use in eq. [6].

Example 6. Taking now the above CC single bond, $\epsilon_6 = 91.56$, as input, we construct a CC single bond, $R = 1.445$ Å (66), like that found in styrene. The change from 1.397 to 1.445 Å translates into $F = -4.98$ with $q_i = q_j = 14.8$ me. Modification of the charge from 14.8 to 7.7 me at the ethylenic carbon, with $a_{CC}^{\sigma} = -0.472$, increases ϵ_{CC} by 3.35, thus giving $\epsilon = 89.93$. Similarly, for 1.48 Å (17) we find $\epsilon_9 = 90.40$ describing the C(Ar)—$C(sp^2)$ reference bond, as in *trans*-stilbene.

Appendix IV

For an aromatic carbon linked to a non-aromatic carbon, $\Sigma_j a_{ij}$ is $2a_{CC}^{\sigma,\pi}(\text{Ar}) + a_{CC}^{\sigma,\pi}(\text{nAr})$, where $a_{CC}^{\sigma,\pi}(\text{Ar})$ is for the benzenic bond and $a_{CC}^{\sigma,\pi}(\text{nAr})$ for the bond formed with a non-aromatic carbon. The change in charge at the aromatic carbon is Δq_C (relative to benzene), contributing $\Delta q_C \Sigma_j a_{ij}$ to ΔE_a^*. On the other hand, this Δq_C is also part of Σq_C, hence, of $\Sigma \Delta q_H$, contributing $-\Delta q_C a_{HC}$. The total contribution of Δq_C is thus

$$[2a_{CC}^{\sigma,\pi}(\text{Ar}) + a_{CC}^{\sigma,\pi}(\text{nAr}) - a_{HC}]\Delta q_C$$

Of course, in this calculation, Δq_C must *not* be included in the evaluation of $\Sigma \Delta q_H$. Using eq. [5], as well as $\Delta q_C = (m + 1) \times \Delta q^{\pi}$ and $\delta = 157\,\Delta q^{\pi}$ (Appendix II), we find that the energy contributed by Δq_C is, in au,

$$m[2a_{CC}^{\sigma}(\text{Ar}) + a_{CC}^{\sigma}(\text{nAr}) - a_{HC}]\left(\frac{\delta}{157}\right)$$

$$+ [2a_{CC}^{\pi}(\text{Ar}) + a_{CC}^{\pi}(\text{nAr}) - a_{HC}]\left(\frac{\delta}{157}\right)$$

where δ is the ^{13}C shift relative to benzene. Inserting the appropriate a_{ij}'s (in au) gives the energy contributed by Δq_C, i.e., in kcal mol^{-1},

$$-(1.2562m + 1.1432)\left(\frac{627.51}{157}\right)\delta = -0.052\,\delta$$

for $m = -0.8997$. It is clear that the final result depends heavily on m, beyond the precision permitted by present SCF charge analyses. Inspection of molecules corresponding to this situation has consistently led to the -0.052 parameter. The corresponding m value, ~-0.90, seems intuitively reasonable when compared to -0.955 for ethylenic carbons (4) and to -0.812 for a benzenic carbon not engaged in a bond with a non-aromatic carbon.

---

[7] Theoretical analyses, at the 4-31G level including polarization functions, account for over 80% of the results anticipated from empirical evaluations (13). Our recipe is, in principle, at the level of experimental accuracy.